

Full Research Paper

Anodic Oxidation and Amperometric Sensing of Hydrazine at a Glassy Carbon Electrode Modified with Cobalt (II) Phthalocyanine–cobalt (II) Tetraphenylporphyrin (CoPc-(CoTPP)₄) Supramolecular Complex

Kenneth I. Ozoemena*

Chemistry Department, University of Pretoria, Pretoria 0002, South Africa

* Author to whom correspondence should be addressed: E-mail: kenneth.ozoemena@up.ac.za;

Received: 11 April 2006 / Accepted: 8 June 2006 / Published: 24 August 2006

Abstract: This paper describes the electrocatalytic behaviour of a glassy carbon electrode (GCE) modified with cobalt(II)phthalocyanine (CoPc) complex peripherally tetrasubstituted with cobalt(II)tetraphenylporphyrin (CoTPP) complexes via ether linkages (i.e., CoPc-(CoTPP)₄). The features of the immobilised pentamer were interrogated with cyclic voltammetry and electrochemical impedance spectroscopy (EIS) using [Fe(CN)₆]^{3-/4-} as redox probe revealed enhanced electron transfer properties with $k_{app} \approx 18 \times 10^{-6} \text{ cm s}^{-1}$ compared to that of the bare GCE ($4.7 \times 10^{-6} \text{ cm s}^{-1}$). The viability of this supramolecular complex as a redox mediator for the anodic oxidation and sensitive amperometric determination of hydrazine in alkaline conditions is described. The electrocatalytic oxidation of hydrazine by GCE-CoPc-(CoTPP)₄ was characterised with satisfactory catalytic current response with low non-Faradaic current (*ca.* 30 times lower than the bare GCE) and at much lower oxidation potential (*ca.* 300 mV lower than the bare GCE). A mechanism for the studied electrocatalytic reaction was proposed based on the spectrophotometric evidence that revealed the major involvement of the Co^(III)/Co^(II) redox couple of the central CoPc species rather than the CoTPP component of the pentamer. Rate constant for the anodic oxidation of hydrazine was estimated from chronoamperometry as $\sim 3 \times 10^3 \text{ M}^{-1} \text{ s}^{-1}$. The proposed amperometric sensor displayed excellent characteristics towards the determination of hydrazine in 0.2 M NaOH; such as low overpotentials (+100 mV vs Ag|AgCl), very fast amperometric response time (1 s), linear concentration range of up to 230 μM , with micromolar detection limit, high sensitivity and stability.

Keywords: Cobalt(II)phthalocyanine-cobalt(II)tetraphenylporphyrin pentamer; Electrochemical impedance spectroscopy; Hydrazine; Anodic oxidation; Amperometric sensor.

1. Introduction

Hydrazine (N_2H_4) is a powerful reducing agent, useful as a fuel in fuel cells [1]. Hydrazine and its derivatives are frequently found in our environment, and are used as essential raw materials and intermediates in some industrial preparations such as pesticides, but also suspected to be carcinogenic and mutagenic [2]. Hydrazine can be absorbed through the skin, affecting our blood production and leading to liver and kidney damage. Thus, it is recognized in pharmacology because of its carcinogenicity and hepatotoxicity. Industrially, hydrazine is commonly employed as a substitute for sulfite in boilers as a scavenger for oxygen. Thus, a highly sensitive method is necessary for the reliable measurement of hydrazine. Several methods including titrimetry [3], coulometry [4], spectrophotometry [5] and electrochemical techniques [6-12] have been described in the literature for the detection of hydrazine. The use of electrochemical sensors are most preferred because of their simplicity, ease of fabrication with excellent possibility for miniaturisation, high sensitivity and reproducibility when compared to other non-electrochemical techniques.

Electrocatalytic oxidation of hydrazine at ordinary electrodes such as the bare carbon electrodes require very large oxidation overpotential. One way to circumvent this problem is the use of chemically modified electrodes (CMEs). Electrodes modified with macrocyclic transition metal complexes such as the metallophthalocyanines (MPcs) have been reported to be efficient catalysts for the oxidation of hydrazine. Metalloporphyrins (red or dark red in solution) and metallophthalocyanines (blue or green in solution) are well recognised supramolecular complexes because of their excellent physico-chemical properties, rich electrochemistry and high versatility as powerful electrocatalysts that could be harnessed for the fabrication of electrochemical sensors [13-16]. The potential technological applications of these molecules will require the use of their thin solid films immobilised onto solid supports such as the glassy carbon electrode (GCE). Individual metallophthalocyanine and metalloporphyrin complexes of cobalt have been reported as efficient electrocatalysts for several molecules of environmental and biomedical relevance such as thiols [17-20], nitric oxide [21-23], nitrite [24] and oxygen [25,26], however, the use of their conjugates in electrocatalysis or electrochemical sensing is grossly under-explored. Recently, the synthesis of a cobalt phthalocyanine covalently linked to four cobalt porphyrin complexes via ether bonds ($CoPc-(CoTPP)_4$) (Fig. 1) was reported [27] with subsequent investigations on its electrocatalytic properties towards the detection of hydrogen peroxide [28] and as redox mediator for glucose oxidase electrode [29]. The electrocatalytic oxidation and detection of hydrazine with cobalt phthalocyanine-based electrodes in strong basic conditions have been reported [8-10]. However, most of the experiments were performed at cathodic potentials. A major disadvantage of cathodic measurements for hydrazine is that oxygen could react with hydrazine in the presence of transition metal ion to generate hydrogen peroxide and nitrogen [30]. Thus, the use of cathodic region is limited by the cathodic reduction of molecular oxygen, which interferes with the reliable hydrazine measurements. Therefore, a sensitive determination of hydrazine in anodic potential window (as described in this work) where oxygen interference is not much of analytical problem is very important.

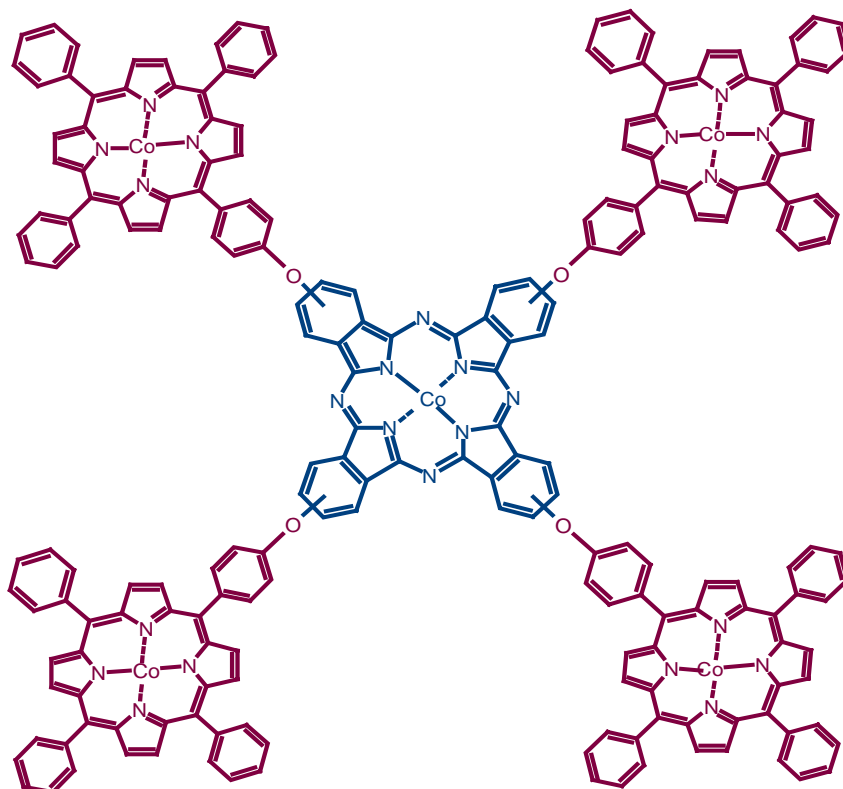


Figure 1: The molecular structure of a cobalt phthalocyanine-cobalt porphyrin (CoPc-(CoTPP)₄) pentamer.

In this work, first, the features of the immobilised CoPc-(CoTPP)₄ were interrogated using cyclic voltammetry and electrochemical impedance spectroscopy (EIS) with [Fe(CN)₆]^{3-/4-} system as a redox probe. Second, the application of the immobilised pentamer film as a viable potential electrocatalyst for both the anodic oxidation and amperometric determination of hydrazine in alkaline pH conditions were studied. Finally, the mechanism of the electrocatalytic processes of hydrazine with the immobilised pentamer film was proposed based on the electrochemistry data and supported by solid UV-visible spectrophotometric investigations. This represents the first report on the use of a metallophthalocyanine-metalloporphyrin conjugate for the study of the electrocatalytic oxidation and detection of hydrazine.

2. Results and Discussion

As described previously [28], GCE-CoPc-(CoTPP)₄ showed a well-defined, and highly electrochemically stable reversible couple in aqueous solution, associated with the [Co^(II)Pc⁽⁻²⁾(TPP⁽⁻²⁾Co^(III))₄/Co^(III)Pc⁽⁻²⁾(TPP⁽⁻²⁾Co^(III))₄] redox process, with a unit ratio of the anodic-to-cathodic peak currents (I_{pa}/I_{pc}), half-wave potential ($E_{1/2} = E_{pa} + E_{pc}/2$) of approximately zero V (vs Ag|AgCl), and a peak-peak separation (ΔE_p) of ~0.2 V (vs Ag|AgCl). In this work, the surface concentration of CoPc-(CoTPP)₄ film attached to the GCE surface was *ca.* 5.0×10^{-10} mol cm⁻². Fig. 2 shows graphical

representation of the effect of the solution pH on the E_p of the $\text{Co}^{\text{(II)}}\text{Pc}^{(-2)}/\text{Co}^{\text{(III)}}\text{Pc}^{(-2)}$ redox couple, studied with SWV. The plot of E_p against pH was linear up to pH 8.0 (E_p (mV) = -53.702 (pH) + 217.79, $r^2 = 0.9929$) but became almost independent from pH 9.0 to 12.0. The slope of -53 mV/pH suggests a monoprotic / monoelectronic redox process. Also, the $\text{Co}^{\text{(III)}}\text{Pc}/\text{Co}^{\text{(II)}}\text{Pc}$ redox couple shifted slightly to the negative potential direction with increasing alkaline pH which may be attributed to the strong binding of the OH^- with the $\text{Co}^{\text{(III)}}\text{Pc}$ [31].

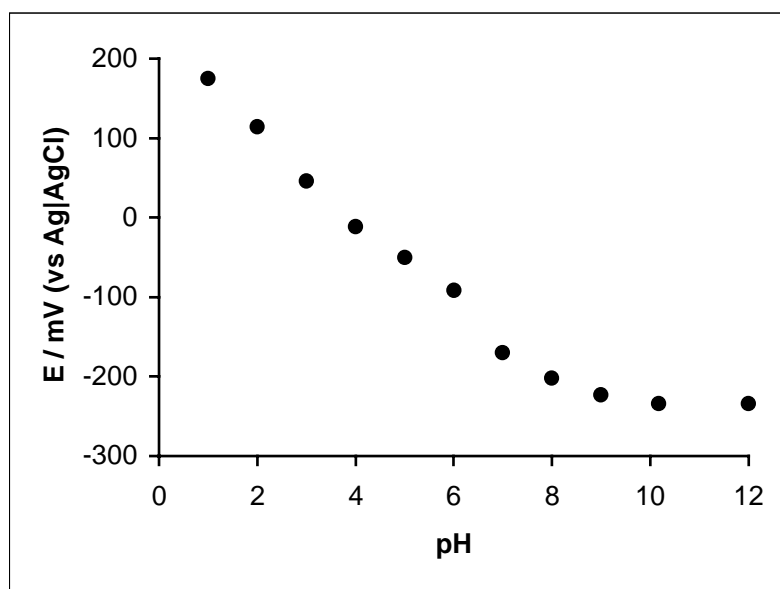


Figure 2: The CV reponse of the GCE-CoPc-(CoTPP)₄ to changes in solution pH.

2.1. Electrochemical impedance spectroscopy studies

Electrochemical impedance spectroscopy (EIS) is an effective technique for probing the features of a surface-confined species [32]. Before the EIS experiments, CVs of the $[\text{Fe}(\text{CN})_6]^{3-/4-}$ redox probe were run. Both GCE and GCE-CoPc-(CoTPP)₄ gave well-defined redox peaks with approximately same current responses. As evident in Fig. 3, the bare GCE showed (Fig. 3 (i)) slightly larger ΔE_p (0.49 V vs Ag|AgCl) compared to that (0.28 V vs Ag|AgCl) obtained for the GCE-CoPc-(CoTPP)₄ (Fig. 3 (ii)). The anodic peak current due to the GCE-CoPc-(CoTPP)₄ was more enhanced and better defined than that shown by the bare GCE. These results clearly showed that the pentamer acts as a redox mediator by enhancing the electronic communication between the GCE and the $[\text{Fe}(\text{CN})_6]^{4-}/[\text{Fe}(\text{CN})_6]^{3-}$ species, possibly by electrostatic attraction of the negatively charged probe and the positively charged cobalt centers of the pentamer. EIS experiments were performed at the formal potential ($E_{1/2} = 0.10$ V vs Ag|AgCl) of $[\text{Fe}(\text{CN})_6]^{3-/4-}$ obtained in Fig.3.

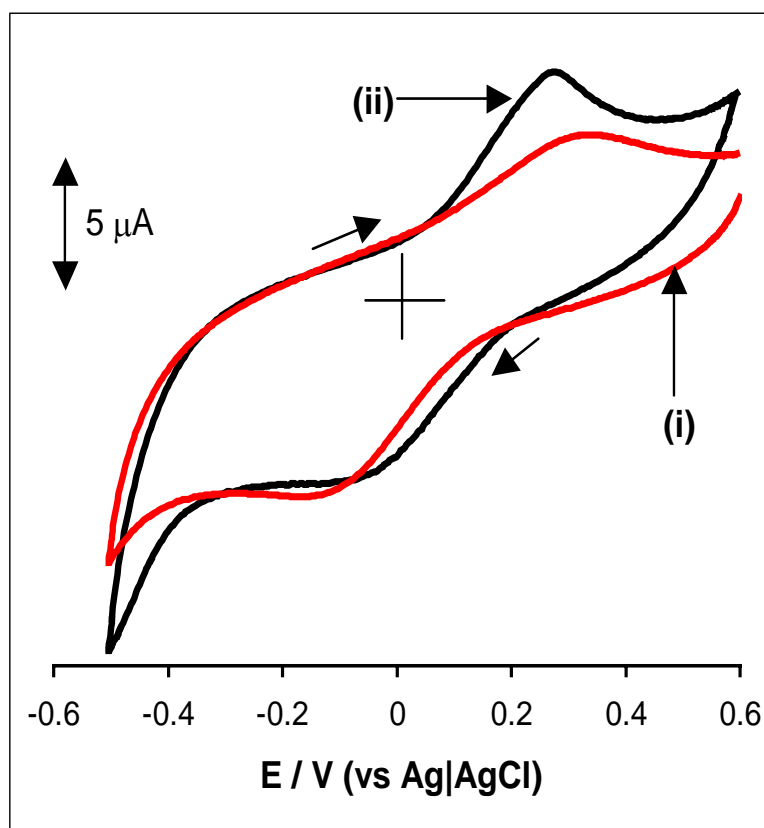


Figure 3: CV response of (i) GCE and (ii) GCE-CoPc-(CoTPP)₄ in 0.1M KCl containing 0.1M KCl containing equimolar mixture of $K_4Fe(CN)_6$ and $K_3Fe(CN)_6$.

The constant phase element (CPE) equivalent circuit model (Fig. 4A), in which the double layer capacitance is replaced by the CPE in Randles' model [32] (i.e., $R_s(CPE[R_{ct}Z_w])$, where R_s is the solution resistance, R_{ct} is the electron-transfer resistance and Z_w is the Warburg impedance) was sufficient to explain the EIS data obtained in this work. The Nyquist plots ($Z_{imaginary}$ vs Z_{real}) (Fig. 4B) exhibited the characteristics semicircles (most pronounced for the bare than the modified GCE) at high frequencies and a straight line at low frequencies, corresponding to kinetic and diffusion processes, respectively. These EIS data (R_s , R_{ct} , CPE and Z_w) were extracted from the Nyquist plots.

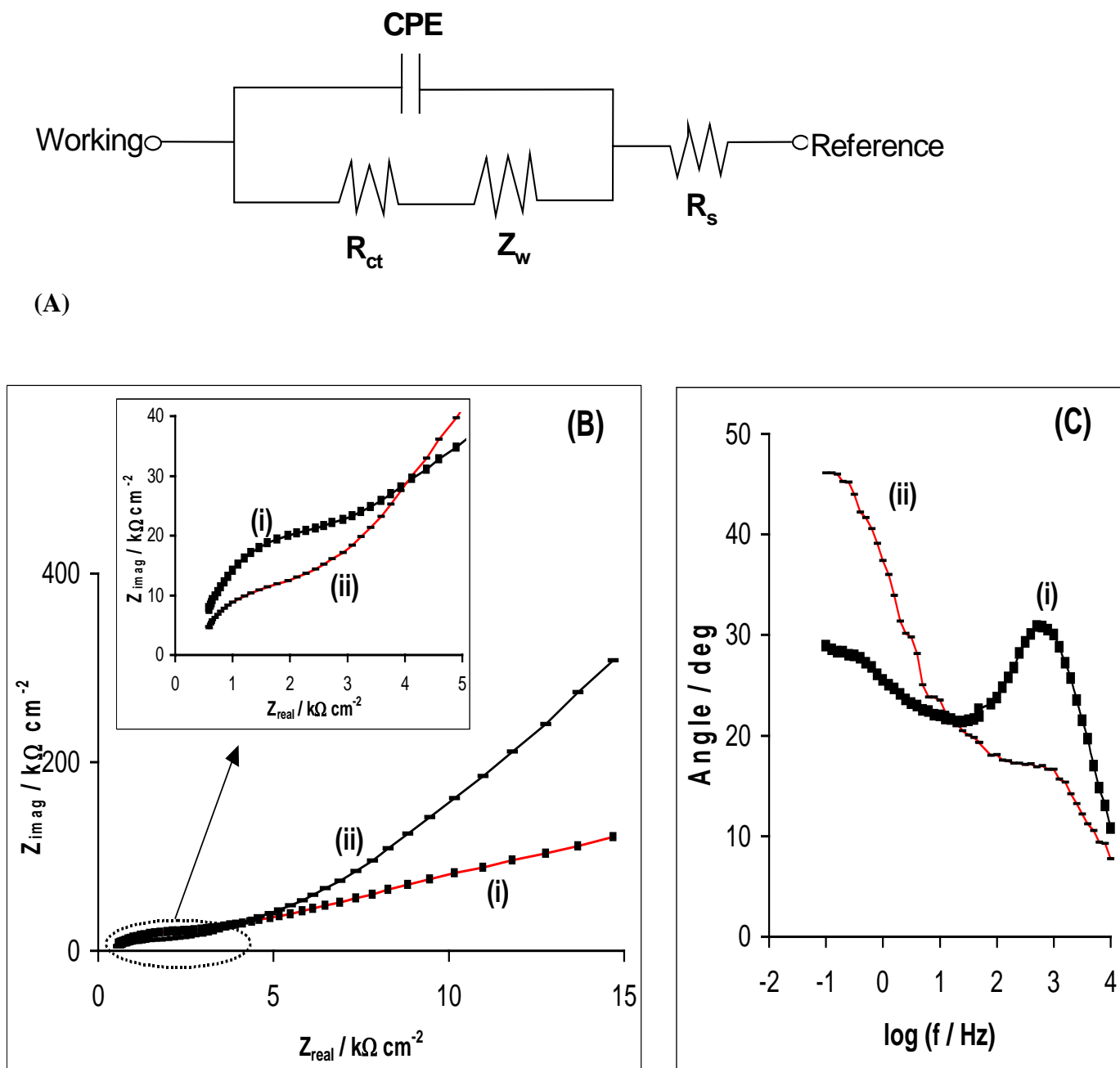


Figure 4: (A) The equivalent circuit model where R_s , R_{ct} , CPE and Z_w represent the solution resistance, the charge transfer resistance, double layer resistance and Warburg impedance, respectively. (B) Nyquist and (C) Bode Plots of (i) GCE and (ii) GCE-CoPc-(CoTPP)₄ in 0.1M KCl containing equimolar mixture of $K_4Fe(CN)_6$ and $K_3Fe(CN)_6$.

For the bare, the R_s , R_{ct} , CPE and Z_w values were estimated as $6.4 k\Omega cm^{-2}$, $56.9 k\Omega cm^{-2}$, $4.0 nF cm^{-2}$ and $12 \times 10^{-4} \Omega cm^{-2} s^{1/2}$, respectively. For the GCE-CoPc-(CoTPP)₄, values of $13.1 k\Omega cm^{-2}$, $14.6 k\Omega cm^{-2}$, $86 nF cm^{-2}$ and $6.4 \times 10^{-4} \Omega cm^{-2} s^{1/2}$ were obtained for the R_s , R_{ct} , CPE and Z_w , respectively. The R_{ct} value for the modified electrodes is approximately a quarter compared to that of the bare GCE, which indicates that the pentamer facilitates the electron transfer process, thus corroborating the CVs of Fig. 3. The slightly higher CPE value for the GCE-CoPc-(CoTPP)₄ reflects the uniformity of the

immobilised film [33], which is somewhat surprising for a drop-dry film. Most probably, the homogeneity might have been attained by pretreatment in the aqueous condition. The apparent electron transfer rate constant k_{app} was obtained from the equation [34]:

$$k_{app} = RT / F^2 R_{ct} C \quad (1)$$

where R is the gas constant ($8.314 \text{ J mol}^{-1} \text{ K}^{-1}$), T is the absolute temperature of the system (298 K), F is the Faraday constant (96485 C mol^{-1}), C is the concentration of the $[\text{Fe}(\text{CN})_6]^{3-}$ (in mol cm^{-3} , the concentration of $[\text{Fe}(\text{CN})_6]^{3-}$ and $[\text{Fe}(\text{CN})_6]^{4-}$ are equal). The calculated k_{app} values for the GCE-CoPc-(CoTPP)₄ ($18.27 \times 10^{-6} \text{ cms}^{-1}$) and the bare GCE ($4.68 \times 10^{-6} \text{ cms}^{-1}$) are of similar magnitude. The high k_{app} value for the GCE-CoPc-(CoTPP)₄ is indicative of faster electron transfer process compared to the bare GCE. It also suggests a small electron-tunnelling distance between the modified film and the GCE, indicating a flat orientation of the pentamer film on the GCE rather than horizontal. From the Bode plots (θ (phase angle) vs $\log f$ (frequency)) (Fig. 4C), the bare GCE showed symmetrical peak with a maximum value of $\sim 31^\circ$ at 631 Hz corresponding to the relaxation process of the GCE|solution interface. Modification of the GCE led to the disappearance of this relaxation with the appearance of an ill-defined maximum ($\sim 46^\circ$ at 0.13 Hz). The disappearance indicates that the reaction takes place at the surface of the CoPc-(CoTPP)₄ film rather than the bare GCE.

2.2. Anodic oxidation of hydrazine

The pKa of hydrazine is known to be 7.9 [35] meaning that most hydrazine is protonated at $\text{pH} < 8.0$. Oxidation of hydrazine with carbon electrodes modified with CoPc and related complexes were performed in strong alkaline pH (0.2 M NaOH) [8-10]. In this work, electrocatalytic oxidation of hydrazine with GCE-CoPc-(CoTPP)₄ exhibited optimum current response at 0.2 M NaOH. Hence, this study was carried out in 0.2 M NaOH conditions. Fig. 5 shows our initial experiment to investigate the current response of the bare GCE (Fig. 5 (i)) and GCE modified with CoPc-(CoTPP)₄ (Fig. 5 (ii)) in 0.2 M NaOH condition. Unlike the bare GCE, the $\text{Co}^{(II)}\text{Pc}/\text{Co}^{(III)}\text{Pc}$ redox couple appeared around -0.10 V (vs Ag|AgCl). The CV showed that this weak redox couple (amplified in the inset) started to appear around -0.20 V (vs Ag|AgCl), very close to where it was observed in Fig. 2 using SWV technique. Fig. 6 shows the voltammetric responses of the GCE-CoPc-(CoTPP)₄ towards the oxidation of hydrazine. The GCE-CoPc-(CoTPP)₄ showed a well-defined anodic oxidation peak at ca $+0.10 \text{ V}$ vs (Ag|AgCl). A broad couple is observed around -0.20 V (vs Ag|AgCl), attributable to $\text{Co}^{(II)}\text{Pc}/\text{Co}^{(III)}\text{Pc}$ couple.

Similar experiments with the bare GCE (Fig. 6 inset) showed hydrazine peak at 0.41 V (vs Ag|AgCl). The integrated peak current response of hydrazine for the bare GCE is approximately equal to that of the GCE-pentamer, however, the pentamer electrode is characterized by a very low background current (ca. 30 times lower than unmodified GCE) and with less positive oxidation peak potential for hydrazine (300 mV lower compared to unmodified GCE). These results confirm that the immobilized CoPc-(CoTPP)₄ solid thin film serves as an efficient electron transfer mediator between hydrazine and the GCE and the pentamer electrode can be successfully employed for the analysis of

this important analyte. Cyclic voltammetric investigation on the influence of different scan rates at constant hydrazine concentration (3×10^{-4} mol/L) (not shown) exhibited catalytic anodic peak current (I_{pa}) values that showed direct proportionality to the square root of scan rate ($v^{1/2}$), indicating a diffusion-controlled reaction. The oxidation of hydrazine in aqueous solution has long been established with EPR to lead to the generation of the radical cation $N_2H_4^+$ [35]. The formation of this radical cation is usually regarded as the rate-determining step since not all proposed intermediates in the oxidation of hydrazine are stable. The plot of the peak potential (E_p) against the logarithm of scan rate ($\log v$) (not shown) resulted in a linear relationship (E_p (V) = $0.0766 (\log v) + 0.2161$, $r^2 = 0.9945$) with a Tafel slope of approximately 153 mV/decade, which suggests that the rate-determining step for the electrocatalysis could follow a one-electron transfer process [36,37]. Tafel slopes greater than the normal 30 – 120 mV/decade for a totally irreversible process such as in this work, have been associated with [38-40] the substrate-catalyst interactions, where the substrate binds very strongly to the catalyst during the interaction as the reaction intermediate step. The Tafel slope obtained in this work may also be rationalized as strong binding of the hydrazine–Pentamer in the intermediate step.

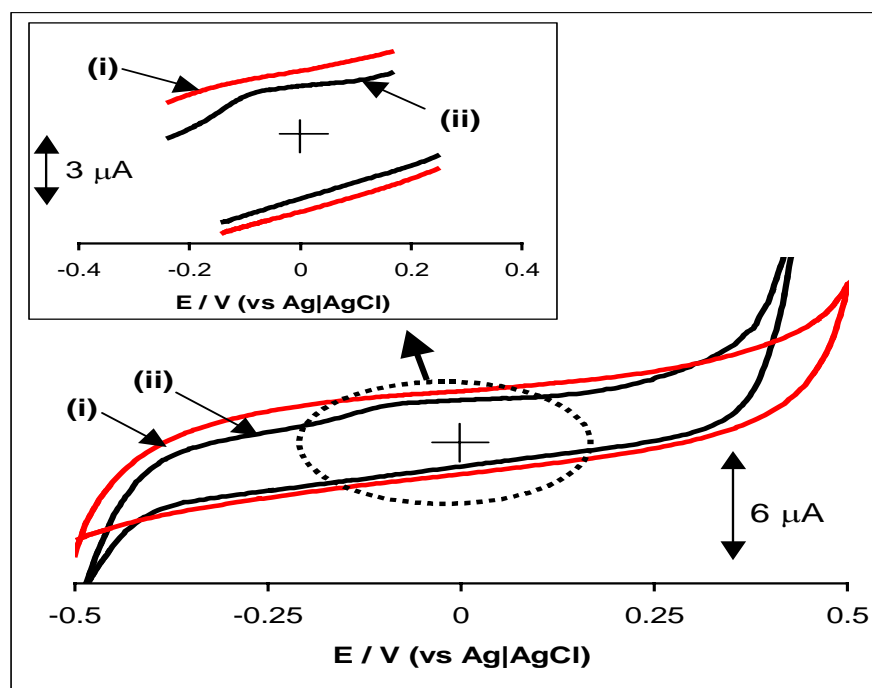


Figure 5: Cyclic voltammograms recorded at (i) bare GCE and (ii) GCE-CoPc-(CoTPP)₄ in 0.2 M NaOH at 25 mVs^{-1} . Inset shows the Co(II)Pc/Co(III)Pc redox couple.

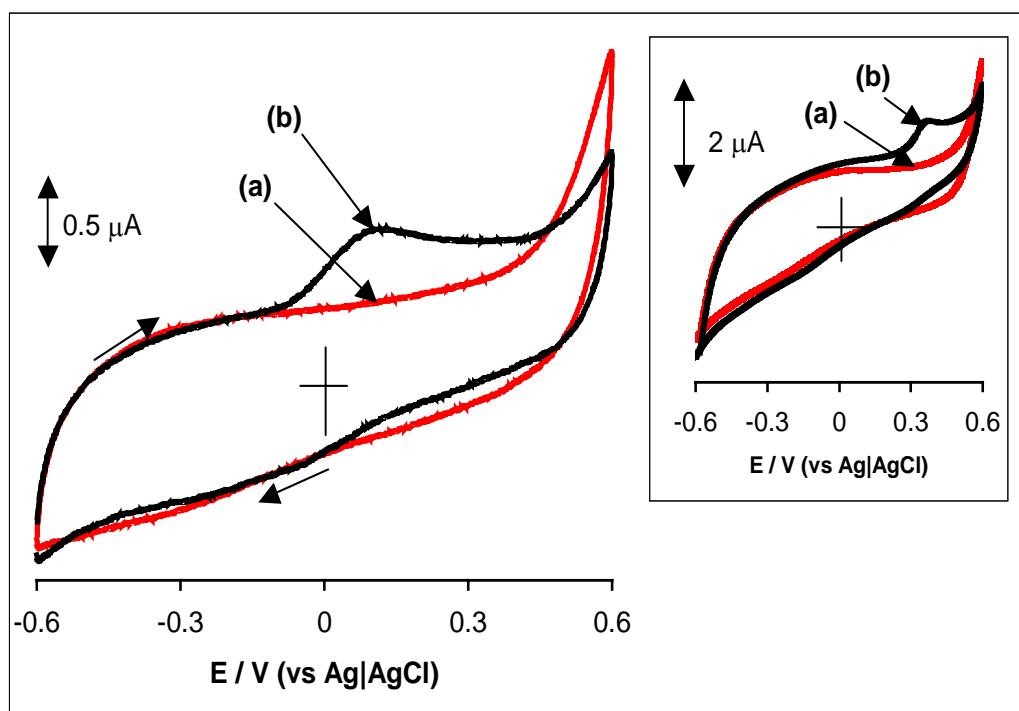


Figure 6: Typical cyclic voltammograms recorded at a GCE-CoPc-(CoTPP)₄ in 0.2 M NaOH without (a) and with (b) 1×10^{-4} mol/L hydrazine at 25 mVs^{-1} . Inset shows the comparative CV responses at bare GCE at the same conditions.

2.3. Proposed mechanism for anodic oxidation of hydrazine

The oxidation of hydrazine started from -0.06 V vs Ag|AgCl, which is close to (-0.2 V vs Ag|AgCl) where the $[\text{Co}^{\text{II}}\text{Pc}^{(-2)}(\text{TPP}^{(-2)}\text{Co}^{\text{III}})_4 / \text{Co}^{\text{III}}\text{Pc}^{(-2)}(\text{TPP}^{(-2)}\text{Co}^{\text{III}})_4]$ redox peak was observed in this alkaline pH condition. This observation confirms the involvement of the $\text{Co}^{\text{III}}/\text{Co}^{\text{II}}$ in this catalytic reaction. Also, it was found that the GCE modified with CoPc film (GCE-CoPc) catalyzed the oxidation of hydrazine at a well-defined peak potential, E_p (-340 mV vs Ag|AgCl) (not shown), which is consistent with reports proposed for the involvement of the $\text{Co}^{\text{III}}\text{Pc}/\text{Co}^{\text{II}}\text{Pc}$ redox couple [9]. Hou et al. [11] had reported before that GCE-CoTPP showed no detectable oxidation peak for hydrazine at $\text{pH} \geq 10$. Thus, the above results further confirm that the operating mechanism for the oxidation of hydrazine involve mainly the central $\text{Co}^{\text{III}}\text{Pc}/\text{Co}^{\text{II}}\text{Pc}$ of this pentamer complex. The involvement of the $\text{Co}^{\text{III}}\text{Pc}/\text{Co}^{\text{II}}\text{Pc}$ couple was further interrogated using solid UV-Vis spectrophotometric investigations. Fig. 7 shows the UV-vis spectra for the CoPc-(CoTPP)₄ when immobilized onto a glass surface(a). This spectrum is similar to the solution spectrum of the pentamer reported previously [27].

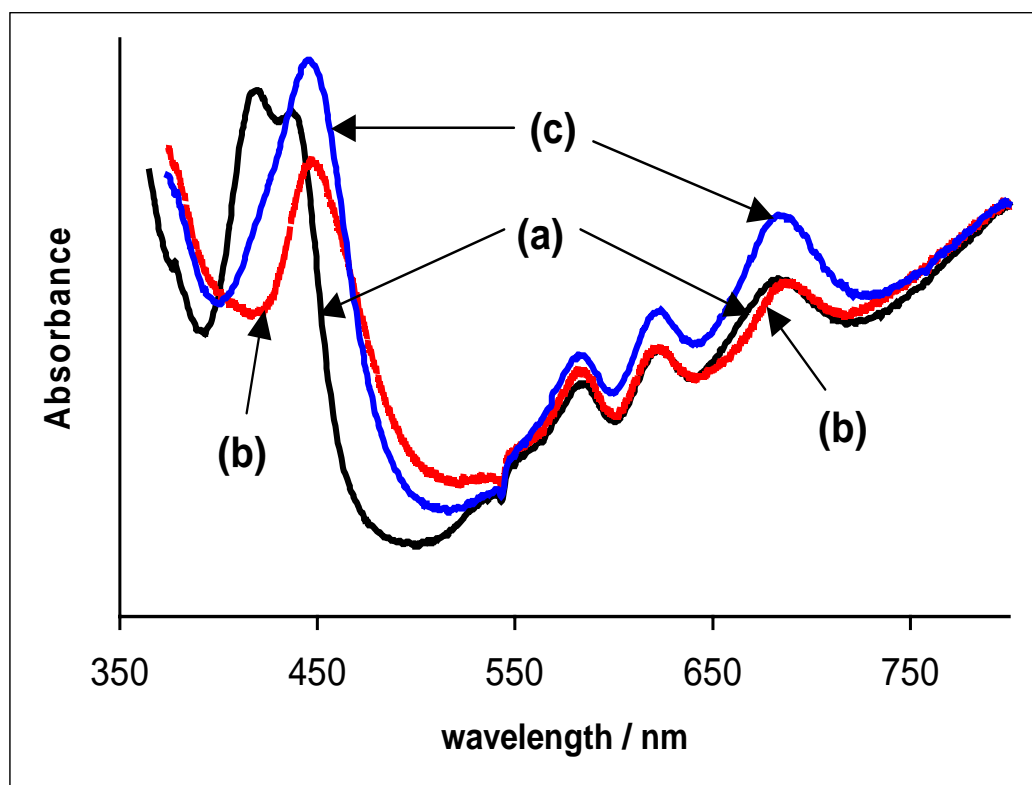


Figure 7: UV-Visible spectra of CoPc-(CoTPP)₄ immobilised at a glass slide (a), after 15 s exposure to bromine vapour (b) and dipping in 0.1 M NaOH solution of hydrazine solution and drying (c).

The split B band (416 and 435 nm) and Q band (580 nm) are due to the CoTPP component of the pentamer while the bands at 618 nm (vibronic) and 680 nm (Q band) are due to the CoPc component of the pentamer. The split B band of the CoTPP is indicative of partial oxidation of the CoTPP from Co(II) to Co(III) [27]. After 15 s exposure to bromine vapour (b), the central Co(II) of both the CoTPP and CoPc are oxidized to their Co(III) species confirmed by the red shifts of the split B band of the CoTPP to a sharp band (442 nm) and Q band of the CoPc (from 680 to 685 nm). Interestingly, on dipping the bromine-oxidised pentamer in a 10^{-3} M solution of hydrazine and then drying (c), the Co(III)Pc (685 nm) quickly reversed to Co(II)Pc (~ 680 nm) while the Co(III)TPP (442 nm) remained unchanged. The inability of the Co(III)TPP to convert to Co(II)TPP further suggests that the central Co^(III)Pc/Co^(II)Pc is the main driving force in the electrooxidation of hydrazine by the pentamer complex. Also, the pentamer-hydrazine spectrum (Fig. 7c) is characterized with higher absorbance, which may suggest improved solubility of the pentamer as a result of coordination with hydrazine. The 5 nm shift to lower wavelength of the Co(III)Pc-hydrazine peak indicates the interaction (most likely axial coordination) of hydrazine to Co^(III)Pc. From the above data, therefore, the main operating mechanism involve the initial oxidation of the central Co^(II)Pc of the pentamer to Co^(III)Pc, followed by

the formation of the hydrazine–Co^(III)Pc adduct and the oxidation of the reduced hydrazine to its products and subsequent regeneration of the Co^(II)Pc species. This is an interesting observation if we consider that electrocatalytic oxidation of hydrazine at basic pH conditions with CoPc-based electrodes generally occur at the cathodic windows and involve the Co^(II)/Co^(I) [8-10] rather than the Co^(III)/Co^(II) redox couple. The reason for the involvement of the Co^(III)/Co^(II) rather than the Co^(II)/Co^(I) redox couple may be attributed to the presence of the four CoTPP appendages of the pentamer, probably by synergistic contribution and the previously established [27] electron-withdrawing influence of the CoTPP on the CoPc. Further electrocatalytic parameters were obtained by carrying out chronoamperometric investigations.

2.4. Chronoamperometric studies

Chronoamperometric investigations were conducted at a 2.15 mM hydrazine. The current for the electrochemical reaction (under mass transport control) of an electroactive analyte such as hydrazine with a diffusion coefficient, D (cm² s⁻¹), is described by the Cottrell equation:

$$I = nFA_{\text{cat}} D^{1/2} C_0 / \pi^{1/2} t^{1/2} \quad (2)$$

assuming $n = 4$ for the complete oxidation of hydrazine in aqueous solution [8-10], and all other parameters retaining their usual meaning and values obtained in this work. From the slope of the linear plot of I vs $t^{1/2}$, D was estimated as 7.30×10^{-8} cm² s⁻¹. This value is less than those (in the $10^{-7} - 10^{-5}$ cm² s⁻¹ range) reported [8,10], which may suggest that the CoPc-(CoTPP)₄ film on the GCE are probably denser than those other electrode modifiers [10].

The heterogeneous rate constant (k), which represents the catalytic reaction rate between the immobilized pentamer film and hydrazine diffusing from the solution, was evaluated using the chronoamperometric approach [6]:

$$I_{\text{cat}}/I_L = (\pi k C_0 t)^{1/2} \quad (3)$$

where I_{cat} and I_L are the current responses of the GCE-CoPc-(CoTPP)₄ in the presence and absence of hydrazine, respectively; k , C_0 and t are the catalytic rate constant (M⁻¹s⁻¹), bulk concentration of hydrazine (M) and time elapsed (s), respectively. From the slope of the plot of the I_{cat}/I_L against $t^{1/2}$ (at intermediate times of 0.5 – 4 s in the present work, exemplified in Fig. 8) for 2.15 mM hydrazine was obtained and k was calculated to be 2.98×10^3 M⁻¹s⁻¹. This value is similar to those reported for other modified electrodes used in the study of electrocatalytic oxidation of hydrazine.

2.5. Chronoamperometric determination of hydrazine

Fig. 9 shows chronoamperograms recorded under stirring (250 rpm) conditions where the potential was poised at +100 mV (vs Ag|AgCl) in 0.2 M NaOH. At this fixed potential (+ 100 mV), a slightly higher current response (~ 7 %) was obtained compared to studies at either +120

or +150 mV, hence all subsequent studies were undertaken at fixed potential of +100 mV (vs Ag|AgCl). As shown in Fig. 9, successive additions of 30 μM , a well-defined response is observed. For each addition of hydrazine, within a fast response time of about one second, a sharp rise in the current was observed. The plot of amperometric response (I_p) vs hydrazine concentration is shown as inset in Fig. 9, giving a linear concentration of 10 – 230 μM . The regression equation of the linear plot was:

$$I_p (\mu\text{A}) = 0.6636 + 0.0157c, \text{ with } r^2 = 0.9991$$

where c is the concentration of hydrazine in μM .

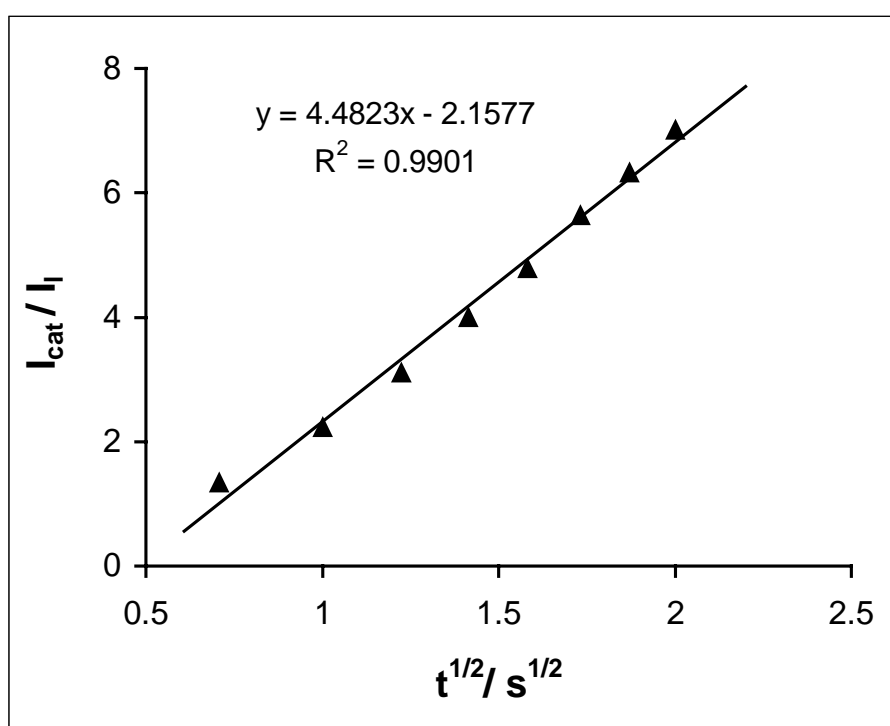


Figure 8: Plot of plot of the I_{cat}/I_L vs $t^{1/2}$

At signal-to-noise ratio of 3, the detection limits were obtained as approximately 1.0 μM . To my knowledge this study represents the first time any metallophthalocyanine-metalloporphyrin conjugate has been used to modify an electrode for the study of the electrocatalytic oxidation and detection of hydrazine. Thus, there are no similar reports with which to adequately compare the present analytical results. A more closer report is the recent study by Li et al. [10] which described the study of hydrazine in 0.2 M NaOH using a GCE that was modified, first with a 4-aminobenzoic acid, alternating layers of diazo-resins (multi-layer film) and a deposit of a water-soluble cobalt tetrasulphophthalocyanine complex and then subjected to UV photochemical reaction. Advantageously, the pentamer-based electrode reported in this work showed linearity at lower concentration range compared to the 5 – 21 mM reported by Li et al [10]. The simplicity of fabrication

of the GCE-CoPc-(CoTPP)₄, requiring less use of chemical reagents, is also of advantage compared to the above report [10].

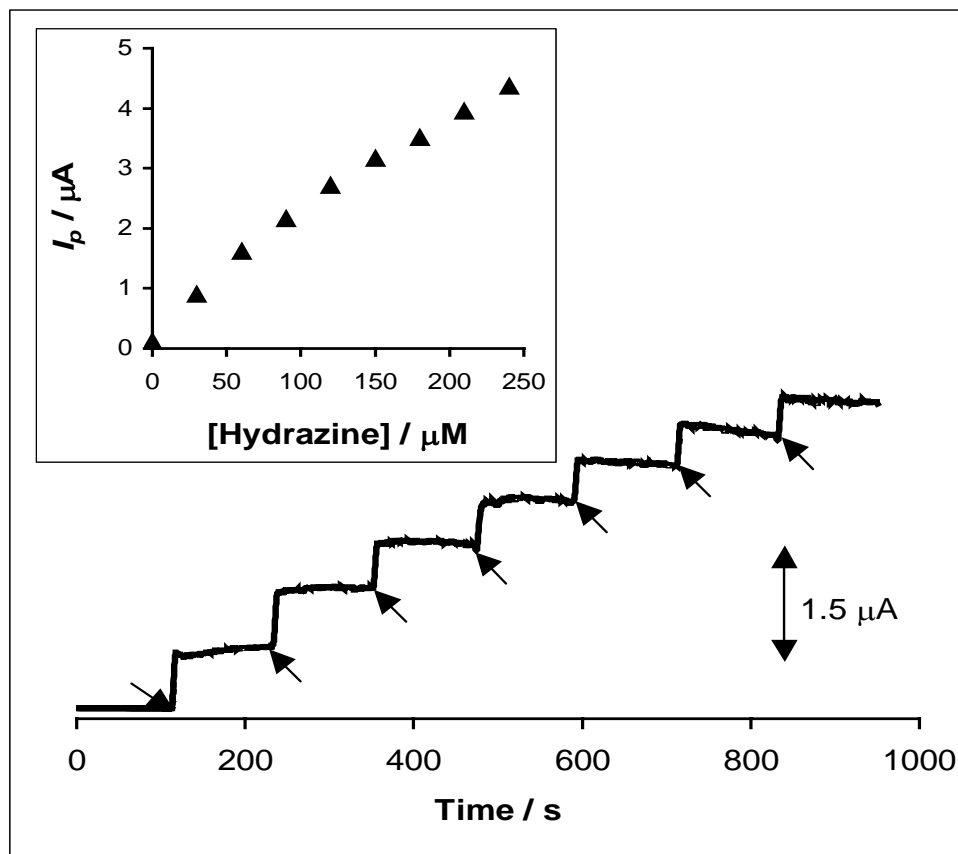


Figure 9: Chronoamperograms recorded at a GCE-CoPc-(CoTPP)₄ on successive additions of 30 μM hydrazine to a 0.2 M NaOH solution. Inset is the corresponding plot of observed current vs hydrazine concentration. Arrows indicate points of injection. Fixed potential = +100 mV (vs Ag |AgCl) ; solution stirred at 250 rpm.

Interference studies were also carried out with the GCE-CoPc-(CoTPP)₄ using a 1:10 (hydrazine:interferent (mol/mol)) ratio. Interestingly, the electrode showed no detectable interference to common species; chloride, bromide, fluoride, carbonate, nitrite, nitrate, sulfate, thiocyanate and hydrogen peroxide under the experimental conditions employed in this work. To assess the suitability of the proposed electrode for potential analytical application, chronoamperometric experiments were also performed with fresh tap water sample (pH adjusted to ~ 12) spiked with hydrazine sulfate using standard addition method. Six replicate determinations showed recovery of 99.82±0.10% of the spike, thus demonstrating the suitability of the proposed CoPc-(CoTPP)₄ based electrode to real sample analysis.

During a multi-scan process in 0.2 M NaOH containing a slightly higher concentration (10⁻⁴ mol/L) of hydrazine, about 30% reduction in the peak height after 80 continuous scans was observed. This

result indicates electrode fouling by the oxidation products of hydrazine during this multi-scan process. But on daily use, the electrode showed good reproducibility (RSD \approx 2%) and good stability for up to one month, a typical behaviour of an electrochemically stable electrode.

2.6. Conclusion

The pentamer shows strong promise for potential application as an efficient redox mediator in the design of an amperometric sensor for hydrazine. Three remarkable results have been revealed by this study. First, CV and EIS data proved that the pentamer-modified GCE is an effective redox mediator. Second, the pentamer film led to the more advantageous anodic oxidation rather than the cathodic oxidation of hydrazine in alkaline conditions. Third, unlike the widely reported cathodic oxidation of hydrazine with CoPc-based electrodes in strong alkaline conditions that involved the $\text{Co}^{\text{(II)}}\text{Pc}/\text{Co}^{\text{(I)}}\text{Pc}$ redox process, the anodic oxidation of hydrazine reported in this work at similar alkaline pH conditions involve $\text{Co}^{\text{(III)}}\text{Pc}/\text{Co}^{\text{(II)}}\text{Pc}$ redox process. Since chronoamperometric detectors are easily integrated with several analytical devices such as the flow injection analysis (FIA), the possible instrumentation designs and technological applications of this amperometric sensor may be found in, for example, the flow-injection analytical system integrated with amperometric detector (FIA-Amp) for environmental and industrial detection and monitoring of hydrazine.

3. Experimental Section

3.1. Reagents and Materials

Cobalt(II) phthalocyanine-cobalt(II) porphyrin ($\text{CoPc}-(\text{CoTPP})_4$) pentamer (Fig. 1) was synthesized from dicyanophenoxy cobalt(II) tetraphenylporphyrin complex and cobalt acetate using the recently reported method [27]. Hydrazine sulphate was obtained from Aldrich. All other reagents were of analytical grades and were used as received from the suppliers without further purification. Ultra pure water of resistivity not less than 18.2 M Ω was obtained from a Milli-Q Water System (Millipore Corp., Bedford, MA, USA) and was used throughout.

3.2. Electrode fabrication and pretreatment

Modification of the glassy carbon electrodes (GCE) with the $\text{CoPc}-(\text{CoTPP})_4$ pentamer and its pretreatment followed our previously reported procedure [28]. Prior to use, the glassy carbon electrode (GCE) was first cleaned by polishing with aqueous slurry of alumina, followed by ultrasonication, rinsed with distilled water and then wiped dry with clean tissue paper. The cleaned GCE was modified by placing a 100 μL of 1 mM DMSO solution of the $\text{CoPc}-(\text{CoTPP})_4$ onto its surface, dried in oven at 80 $^\circ\text{C}$ for 2 hr and finally allowed to cool to room temperature. When dried, the original green solution of the pentamer on the GCE surface turned to a blue-purple thin film. The modified electrode is thoroughly rinsed in water and then immersed in a 0.1 M HClO_4 electrolyte solution and the potential was repetitively cycled from -0.60 to +0.60 V (vs $\text{Ag}|\text{AgCl}$) at 25 mVs^{-1} until a stable reversible voltammogram was obtained. When not in use, the electrode was stored in a refrigerator.

Electrochemical data (voltammograms and chronoamperograms) were obtained with BioAnalytical System (BAS) 100 B/W Electrochemical Workstation, using a conventional three-electrode set-up with a 3.00 mm diameter GCE (BAS) modified with CoPc-(CoTPP)₄ (herein referred to as GCE-CoPc-(CoTPP)₄) as a working electrode, platinum wire as a counter electrode and Ag|AgCl wire as a pseudo-reference electrode. Electrochemical impedance spectroscopy (EIS) measurements were performed with an Autolab FRA software between 100 mHz and 10 kHz using a 10 mV rms sinusoidal modulation in a solution of 1 mM of K₄Fe(CN)₆ and 1 mM K₃Fe(CN)₆ (1:1) mixture containing 0.1 M KCl, and at the E_{1/2} of the [Fe(CN)₆]^{3-/4-} (0.1 V vs Ag|AgCl). Anodic oxidation and detection of the hydrazine was performed in 0.2 M NaOH solution (pH ~ 12). The pH studies were performed with 0.1 M phosphate buffer solutions, the required pH adjusted appropriately using a 10 mM M NaOH or H₃PO₄ solutions. A WTW pH 330/SET-1 (Germany) pH meter was used for pH measurements. Chronoamperometric sensing of hydrazine was carried out in stirred (250 rpm) solution with potential fixed at +100 mV (vs Ag|AgCl). Tap water sample was obtained from public tap water and was analysed on the same day using the chronoamperometry. The pH of the tap water was adjusted to from pH 7.03 to about pH 12 using 0.01M NaOH. A Wissenschaftlick-Technische Werkstätten (WTW) pH 330/SET-1 (Germany) pH meter was used for pH measurements. All experiments were performed at room temperature, 25±1 °C.

Acknowledgements

The financial support of the National Research Foundation of South Africa (NRF, GUN 2073666) for this work is acknowledged. Useful discussions with Prof. Tebello Nyokong (Rhodes University) on this manuscript are highly appreciated.

References

1. Yamada, K.; Yasuda, K.; Fujiwara, N.; Siroma, Z.; Tanaka, H.; Miyazaki, Y.; Kobayashi, T. Potential application of anion-exchange membrane for hydrazine fuel cell electrolyte. *Electrochem. Commun.* **2003**, *5*, 892-896.
2. Poso, A.; von Wright, A.; Gynther, J. An empirical and theoretical study on mechanisms of mutagenic activity of hydrazine compounds. *Mutation Res.* **1995**, *332*, 63–71.
3. Huamin, J.; Weiyang, H.; Erkany, W. Amperometric flow-injection analysis of hydrazine by electrocatalytic oxidation at cobalt tetraphenylporphyrin modified electrode with heat treatment. *Talanta* **1992**, *39*, 45-50
4. Malaki, E.A.; Koupparis, M.K. Kinetic study of the determination of hydrazines, isoniazid and sodium azide by monitoring their reactions with 1-fluoro-2,4-dinitrobenzene, by means of a fluoride-selective electrode, *Talanta* **1989**, *36*, 431-436
5. Dias, F.; Olojola, A.S.; Joselskis, B. Spectrophotometric determination of micro amounts of hydrazine and hydroxylamine alone and in the presence of each other. *Talanta* **1979**, *26*, 47-49.
6. Pournaghi-Azar, M.H.; Sabzi, R. Electrochemical characteristics of a cobalt pentacyanonitrosylferrate film on a modified glassy carbon electrode and its catalytic effect on the electrooxidation of hydrazine. *J. Electroanal. Chem.* **2003**, *543*, 115-125

7. Ozoemena, K.I.; Nyokong, T. Electrocatalytic oxidation and detection of hydrazine at gold electrode modified with iron phthalocyanine complex linked to mercaptopyrindine self-assembled monolayer. *Talanta* **2005**, *67*, 162-168.
8. Zhang, J.; Tse, Y-H.; Pietro, W.J.; Lever, A.B.P. Electrocatalytic activity of NNNN-tetramethyltetra-3,4-pyridoporphyrazinocobalt(II) adsorbed on a graphite electrode towards the oxidation of hydrazine and hydroxylamine. *J. Electroanal. Chem.* **1996**, *406*, 203-211.
9. Isaacs, M.; Aguirre, M.J.; Toro-Labbe, A.; Costamagna, J.; Paez, M.; Zagal, J.H. Comparative study of the electrocatalytic activity of cobalt phthalocyanine and cobalt naphthalocyanine for the reduction of oxygen and the oxidation of hydrazine. *Electrochim. Acta* **1998**, *43*, 1821-1827
10. Li, X.; Zhang, S.; Sun, C. Fabrication of covalently attached multiplayer film electrode containing cobalt phthalocyanine and its electrocatalytic oxidation of hydrazine. *J. Electroanal. Chem.* **2003**, *553*, 139-145.
11. Hou, W.; Ji, H.; Wang, E. Amperometric flow-injection analysis of hydrazine by electrocatalytic oxidation at cobalt tetraphenylporphyrin-modified electrode with heat treatment. *Talanta* **1992**, *39*, 45-50
12. Batchelor-McAuley, C.; Banks, C.E.; Simm, A.O.; Jones, T.G.J.; Compton, R.G. A comparison of the use of palladium nanoparticles supported on a boron-doped diamond and palladium plated BDD microdisc array. *Analyst* **2006**, *131*, 106-110.
13. Kadish, K.M.; Smith, K.M.; Guillard, R. Eds.; *The Porphyrin Handbook*, Vol.1-20, Academic Press, Boston, **1999-2003**.
14. Vasuvedan, P.; Poughat, N.; Shuklat, A.K. Metal phthalocyanines as electrocatalysts for redox reactions. *Appl. Organomet. Chem.* **1996**, *10*, 591-604.
15. Ozoemena, K.I.; Nyokong, T. In *Encyclopedia of Sensors*, C. A Grimes, E.C.; Dickey, M.V., Pishko, Eds.; American Scientific Publishers: California, 2006; Vol. 3, Chapter E, p.157-200.
16. Bedioui, F.; Devynck, J.; Bied-Charreton, C. Immobilization of metalloporphyrins in electropolymerized films: design and applications. *Acc. chem. Res.* **1995**, *28*, 30-36.
17. Zagal, J.H.; Gulppi, M.A.; Caro, C.A.; Cárdenas-Jirón, G.I. Paradoxical effect of the redox potential of adsorbed metallophthalocyanines on their activity for the oxidation of 2-mercaptoethanol. Inner versus outer sphere electrocatalysis. *Electrochem. Commun.* **1999**, *1*, 389-393.
18. Ozoemena, K.I.; Nyokong, T.; Westbroek, P. Self-assembled monolayers of cobalt and iron phthalocyanine complexes on gold electrodes: Comparative surface electrochemistry and electrocatalytic interaction with thiols and thiocyanate. *Electroanalysis* **2003**, *15*, 1762-1770.
19. Griveau, S.; Gulppi, M.; Bedioui, F.; Zagal, J.H. Electropolymerized cobalt macrocomplex-based films for thiols electro-oxidation: effect of the film formation conditions and the nature of the macrocyclic ligand. *Solid State Ionics*, **2004**, *169*, 59-63.
20. Maree, S.; Nyokong, T. Electrocatalytic behavior of substituted cobalt phthalocyanines towards the oxidation of cysteine. *J. Electroanal. Chem.* **2000**, *492*, 120-127.
21. Nyokong, T.; Vilakazi, S. Phthalocyanines and related complexes as electrocatalysts for the detection of nitric oxide. *Talanta* **2003**, *61*, 27-35.

22. Oni, J.; Diab, N.; Radtke, I.; Schuhmann, W. Detection of NO release from endothelial cells using Pt micro electrodes modified with a pyrrole-functionalised Mn(II) porphyrin. *Electrochim. Acta* **2003**, *48*, 3349-3354.
23. Pereira-Rodrigues, N.; Albin, V.; Koudelka-Hep, M.; Auger, V.; Pailleret, A.; Bedioui, F. Nickel tetrasulfonated phthalocyanine based platinum microelectrode array for nitric oxide oxidation. *Electrochem. Commun.* **2002**, *4*, 922-927.
24. Cosnier, S.; Gondran, C.; Wessel, R.; Montforts, F-P.; Wedel, M. A poly(pyrrole-cobalt(II)deuteroporphyrin) electrode for the potentiometric determination of nitrite, *Sensors* **2003**, *3*, 213-222
25. D'Souza, F.; Hsieh, Y.Y.; Wickman, H.; Kutner, W.; New sensor for dissolved dioxygen: a gold electrode modified with a condensation polymer film of β -cyclodextrin hosting cobalt tetraphenylporphyrin. *Chem. Commun.* **1997**, 1191-1192.
26. Tse, Y-H.; Janda, P.; Lam, H.; Pietro, W.J.; Lever, A.B.P. Monomeric and polymeric tetraaminophthalocyaninatocobalt(II) modified electrodes: electrocatalytic reduction of oxygen. *J. Porphyrins phthalocyanines* **1997**, *1*, 3-16.
27. Zhao, Z.X.; Ozoemena, K.I.; Maree, D.M.; Nyokong, T. Synthesis and electrochemical studies of a covalently linked cobalt(II) phthalocyanine-cobalt(II) porphyrin conjugate. *Dalton Trans.* **2005**, 1241-1248.
28. Ozoemena, K.I.; Zhao Z.X.; Nyokong, T. Immobilized cobalt (II) phthalocyanine-cobalt (II) porphyrin pentamer at a glassy carbon electrode: Applications to efficient amperometric sensing of hydrogen peroxide in neutral and basic media. *Electrochem. Commun.* **2005**, *7*, 679-684
29. Ozoemena K.I.; Nyokong, T. Novel amperometric glucose biosensor based on an ether-linked cobalt(II) phthalocyanine-cobalt(II) tetraphenylporphyrin pentamer as a redox mediator. *Electrochim. Acta* **2006**, *51*, 5131-5136.
30. Mantai, K.E.; Hind, G. Mechanism and stoichiometry of the oxidation of hydrazine by illuminated chloroplasts. *Plant Physiol.*, **1971**, *48*, 5-8.
31. Nevin, W.A.; Hempstead, M.R.; Liu, W.; Leznoff C.C.; Lever, A.B.P. Electrochemistry and spectroelectrochemistry of mononuclear and binuclear cobalt phthalocyanines. *Inorg. Chem.* **1987**, *26*, 570-578.
32. Katz E.; Wilner, I. In Ultrathin Electrochemical Chemo- and Biosensors. Technology and Performance; Mirsky, V.M. Ed; Springer-Verlag; New York, 2004; Chapter 4, p.68-116.
33. Bisquert, J.; Garcia-Belmonte, G.; Bueno, P.; Longo, E.; Bulhoes, L.O.S. Impedance of constant phase element (CPE)-blocked diffusion in film electrodes. *J. Electroanal. Chem.* **1998**, *452*, 229-234
34. Sabatini, E.; Rubinstein, I. Organized self-assembled monolayers on electrodes. 2. Monolayer-based ultramicroelectrodes for the study of very rapid electrode kinetics. *J. Phys. Chem.* **1987**, *91*, 6663-6669.
35. Adams, J.Q.; Thomas, J.R. Electron Paramagnetic Resonance of a Hydrazine Radical Ion. *J. Chem. Phys.* **1963**, *39*, 1904-1906
36. Zhao, Y.-D.; Zhang, W.-D.; Chen, H.; Luo, Q.-M. Anodic oxidation of hydrazine at carbon nanotube powder microelectrode and its detection. *Talanta* **2002**, *58*, 529-534.

37. Golabi, S.M.; Zare, H.R.; Hamzehloo, M. Electrocatalytic oxidation of hydrazine at a pyrocatechol violet (PCV) chemically modified electrode. *Microchem. J.* **2001**, *69*, 13-23.
38. Zen, J.-M.; Kumar, A. S.; Chang, M.-R. Electrocatalytic oxidation and trace detection of amitrole using a Nafion/lead–ruthenium oxide pyrochlore chemically modified electrode. *Electrochim. Acta* **2000**, *45*, 1691-1700.
39. Wermeckers, B.; Beck, F.; Anodic oxidation of β -cyanoethyl ethers. *Electrochim. Acta* **1985**, *30*, 1491-1500
40. Siswana, M.; Ozoemena, K.I.; Nyokong, T. Electrocatalytic behaviour of carbon paste electrode modified with iron (II) phthalocyanine (FePc) nanoparticles towards the detection of amitrole. *Talanta* **2006**, *69*, 1136-1142.